Conformation of the γ Subunit at the $\gamma-\epsilon-c$ Interface in the Complete *Escherichia coli* F_1-ATPase Complex by Site-Directed Spin Labeling†

Scott H. Andrews, Yelena B. Peskova, Mark K. Polar, Vincent B. Herlihy, and Robert K. Nakamoto*

Department of Molecular Physiology and Biological Physics, University of Virginia, P.O. Box 800736, Charlottesville, Virginia 22908-0736

Received July 6, 2001

ABSTRACT: Structure−function relationships of the $\gamma-\epsilon-c$ subunit interface of F_OF_1 ATP synthase, a region of subunit interactions important in coupling between catalysis and transport, were investigated by site-directed spin labeling and electron paramagnetic resonance (EPR) spectroscopy. The EPR line widths and collision accessibilities of 18 spin-labeled, unique cysteine F_1 mutants from γLeu198 to γLeu215 indicate an alternating pattern in the mobility and accessibility parameters for positions γ201−209, which is reminiscent of a β-strand. Labels at positions γ204 and γ210 show tertiary contact upon F_1 binding to F_O and γD210C has reduced coupling efficiency. γE208C could not be spin labeled, but the uncoupling effects of γE208K are suppressed by second-site mutations in the polar loop of subunit *c* [Ketchum, C. J. and Nakamoto, R. K. (1998) *J. Biol. Chem. 273*, 22292−22297]. The restricted mobility and accessibility of spin labels in the odd-numbered positions between γ201 and γ207 plus the 2−4-fold higher values in k_{cat} for ATP hydrolysis of these same mutant F_1 indicate that the interactions of these residues with the ϵ subunit mediate its inhibitory activity. Disrupted interactions with ϵ subunit also cause reduced coupling efficiency. We propose a model for the $\gamma-\epsilon-c$ interface of *Escherichia coli* F_OF_1 ATP synthase in which side chains from the odd-numbered residues of the γLys201−γTyr207 β-strand directly and functionally interact with the ϵ subunit, while the even-numbered, acidic residues γAsp204, γGlu208, and γAsp210 interact with the F_O sector, probably with subunit *c*. γ Subunit interactions with both subunits in this region are important for coupling efficiency.

The F_OF_1 ATP synthase couples translocation of protons in the membranous F_O sector to synthesis or hydrolysis of ATP in the soluble F_1 sector through a mechanism that includes rotation of the γ, ϵ, and *c* subunits relative to $\alpha_3\beta_3\delta b_2 a$ (*1*−*3*). Energy coupling involves conformational information transmitted through the three rotor subunits γ, ϵ, and *c* (reviewed in refs *4* and *5*). This communication is disrupted by mutations in a segment of the γ subunit that perturb interactions with the ϵ and *c* subunits, including γY205C, which abrogates ϵ inhibition of F_1 and disrupts coupling between F_O and F_1 (*6*, *7*), and γE208K, which disrupts coupling without affecting ϵ inhibition (*7*, *8*).

Two recent high-resolution crystal structures detailed the F_1 components of the $\gamma-\epsilon-c$ interface, in bovine mitochondrial F_1 (*9*), and in an *Escherichia coli* F_1 construct containing the ϵ subunit and a truncated γ subunit (γ'), but no α, β, or δ subunits (*10*). The γ'/ϵ structure showed a strand of alternating residues from γTrp203 to γPro209 facing the ϵ subunit, followed by a turn and the long carboxyl terminal helix extending from γPro211, but failed to resolve γPro191 to γLeu198 (*10*). The complete structure of bovine mitochondrial F_1 (*9*) showed a different local conformation, which is not surprising considering the low similarity between these isoforms in this region.

To examine structure−function relationships of this region of *E. coli* F_OF_1 ATP synthase, and ultimately the mechanism of energy coupling, we began structural and functional analyses of cysteine substitutions in the γ subunit using the site-directed spin labeling (SDSL)[1] strategy of electron paramagnetic resonance (EPR) spectroscopy (reviewed in ref *11*) The resulting EPR data obtained in a full *E. coli* F_1 complex confirm the secondary and tertiary structure assignments of the γ'/ϵ structure (*10*) and identify the functionally important $\gamma-\epsilon$ or $\gamma-F_O$ interactions that mediate ϵ subunit inhibition and modulate the catalytic mechanism to achieve efficient coupling between transport and catalysis.

EXPERIMENTAL PROCEDURES

Strains and Plasmids. ATP synthase mutants, with all native cysteines replaced by alanine and a Flag affinity tag (Sigma Chemical Co., St. Louis, MO) at the amino terminus of the β subunits, were expressed from plasmid-borne *unc* operon on pACWU1.2/βFlag/ΔCys (*12*) in strain DK8 (*bglR thi-1 rel-1 HfrPO1* Δ*(uncB−uncC) ilv::Tn10;* (*13*)). Cysteine substitutions from γLeu198 to γLeu215 were introduced by polymerase chain reaction (*14*) with the *Pfu* thermophilic polymerase (Stratagene, La Jolla, CA) in plasmid pBγKS

† This work was supported by United States Public Health Service Grant GM50957. S.H.A. was supported by a postdoctoral fellowship from the Cardiovascular Training Grant, NIH HL07284.

* To whom correspondence should be addressed. Tel: 434-982-0279. Fax: 434-982-1616. E-mail: rkn3c@virginia.edu.

[1] Abbreviations: SDSL, site-directed spin labeling; EPR, electron paramagnetic resonance; NiEDDA, nickel (II) ethylenediamine-*N*,*N*′-diacetic acid; MTS-SL, methanethiosulfonate 1-oxyl-2,2,5,5-tetramethyl-Δ^3-pyrroline-3-methyl; DTT, dithiothreitol; TCEP, tris-(2-carboxyethyl) phosphine.

10.1021/bi0155697 CCC: $20.00
Published on Web 08/08/2001

(*12*). After sequencing of the entire insert, the *Rsr*II−*Spe*I fragment was ligated into pACWU1.2/βFlag/ΔCys (*12*). The single cysteine mutant strains exhibited growth comparable to that of cysteine-less F_OF_1 on sodium succinate, a nonfermentable carbon source requiring a functional F_OF_1 ATP synthase for growth. Wild-type and cysteine-less F_OF_1 ATP synthase were expressed in strain DK8 from plasmid-borne *unc* operon on pACWU1.2/βFlag and pACWU1.2/βFlag/ΔCys (*12*), respectively.

Recombinant, polyhistidine tagged ϵ subunit (His-ϵ) was expressed in strain BL21(DE3)*pLysS* (Novagen, Madison, WI). The polyhistidine tag was added by PCR amplification of *uncC* with the following oligonucleotide primers, which introduced *Nco*I and *EcoR*I restriction sites at the 5′ and 3′ ends of *unc*C, respectively: 5′-ACTCCATGGCAATGACTTACCACCTGG-3′ and 5′-ATCGAATTCAGAGTCAAACCGCTTCACCTTG-3′. The entire insert was sequenced and ligated into pHIS−Parallel1 (*15*). This vector added the amino terminal $(His)_6$ and rTEV protease site sequence, MSYYHHHHHHDYDIPTTENLYFQGA, preceding the *uncC* open reading frame.

Molecular biology protocols were performed according to the manufacturers' instructions or by Sambrook et al. (*16*). DNA-modifying and restriction enzymes were obtained from New England Biolabs (Beverly, MA), Gibco-BRL (Rockville, MD), or Roche Molecular Biochemicals (Indianapolis, IN).

Enzyme Preparations. F_OF_1-containing membranes were prepared by growth of strains until mid-log phase in minimal medium (*17*) supplemented with 1.1% glucose at 37 °C and isolated as previously described (*18*). Flag-F_1 enzymes were purified as previously described (*8*) in 1.0−1.3 mg yields of purified F_1 per liter of culture. SDS−PAGE (*19*) of purified F_OF_1 or F_1 mutants showed qualitatively correct amounts of all F_OF_1 or F_1 subunits, including ϵ. Membranes enriched in wild-type F_O were purified as above and stripped of F_1 as previously described (*18*). Reconstitution of hybrid F_OF_1 complexes were prepared by mixing 0.75 mg of purified F_1, or spin-labeled purified F_1, with 0.56 mg of F_O-containing membranes (approximately a 5:1 molar excess of F_1 over F_O). The mixtures were incubated for 10 min on ice, centrifuged at 576000*g* for 60 min, the membrane pellet washed in 50 mM Tris-HCl, 10% (v/v) glycerol, 2 mM $MgCl_2$, 1 mM ATP, 40 mM 6-aminohexanoic acid, 40 mM Na_2SO_4, pH 7.4, centrifuged again, and the membrane pellet was suspended in the above buffer. Prior to proton pumping assays, membranes containing hybrid F_OF_1 were suspended at 10 mg/mL into 10 mM Tris-HCl, 140 mM potassium chloride, and 10% (v/v) glycerol, pH 8.0, and used in the assay as described in the legend to Figure 3. Purified F_1, F_OF_1, and F_O enriched membranes were assayed for concentration by the method of Lowry et al. (*20*).

Preparation of Recombinant ϵ Subunit. His-ϵ was expressed on minimal media supplemented with 1.1% glucose by induction with isopropyl β-D-thiogalactopyranoside at mid-log phase for 2 h. Cells were harvested and solubilized in buffer A (20 mM Tris-HCl, 100 mM NaCl, pH 8.0), passed through a French pressure cell twice, and the insoluble lysate fraction was removed by ultracentrifugation.

His-ϵ was isolated from the soluble lysate on a Talon affinity column (Clontech, Palo Alto, CA), followed by washes of buffer A and elution in buffer A plus 100 mM imidazole. The polyhistidine tag was removed by incubation with rTEV protease (Life Technologies, Gaithersburg, MD) for 4 h at room-temperature plus 24 h at 4 °C. Excess imidazole was removed by dialysis against buffer A, and the protease and $(His)_6$ fragment were removed by passage over Talon resin. Purity of cleaved recombinant ϵ was confirmed by SDS−PAGE (*19*), and activity was determined by inhibition of diluted, ϵ-depleted wild-type F_1 (data not shown) under assay conditions previously reported (*7*). His-ϵ in buffer A plus 10% (v/v) glycerol was concentrated by ultrafiltration on a Centricon 3 filter (Millipore, Bedford, MA) to approximately 350 μM. Yield of purified His-ϵ was 1−2 g per liter of culture.

Enzymatic Assays. The k_{cat} of ATP hydrolysis was obtained in a buffer containing 50 mM HEPES−KOH, 10 mM ATP, 5 mM $MgCl_2$, and 1 μM carbonyl cyanide *m*-chlorophenylhydrazone (in assays of membrane preparations) at 30 °C, pH 7.5, with 5 mM phosphoenolpyruvate and 50 mg/mL pyruvate kinase (*7*). In assays of F_1, the concentration of enzyme was 25 nM, above the K_D for ϵ subunit (3 nM) to keep the subunit bound to the complex (*7*, *21*). ATP synthesis (*22*) and proton pumping (*23*) were performed as previously described.

Spin Labeling and EPR Spectroscopy. F_1 mutants in 50 mM Tris-HCl, 10% (v/v) glycerol, 2 mM $MgCl_2$, 1 mM ATP, 40 mM 6-aminohexanoic acid, 40 mM Na_2SO_4, pH 7.4, were concentrated to approximately 20 μM by ultra-filtration on a Centricon 10 filter (Millipore, Bedford, MA) and spin labeled overnight using a 5−10 molar excess of methanethiosulfonate spin label (MTS−SL). Unreacted MTS−SL was removed by filtration through 1-mL Sephadex G-50 centrifuge columns (*24*), and the effluent was concentrated to approximately 40 μM by ultrafiltration. Some samples were treated during the initial concentration with 10 molar equivalents of dithiothreitol (DTT), which was removed immediately prior to spin labeling by Sephadex column filtration as above. F_1 mutants for use in hybrid F_OF_1 were reacted as above for 1 h. Stoichiometry of labeling was determined in selected samples by comparison of protein concentration with spin concentration, the latter determined by double integration of the EPR derivative spectra and comparison to the double integrals of a series of known concentration standards containing 3-carboxy-PROXYL nitroxide (Aldrich Chemical Co., Milwaukee, WI).

EPR data were obtained on a Bruker 300 Series spectrometer with a Loop-Gap resonator (Medical Advances, Milwaukee, WI). Spectra were taken at 100 G field sweep, 1 G modulation amplitude, and 2 mW power. Power saturation samples were placed in TPX plastic capillaries (Medical Advances, Milwaukee, WI) and flushed with nitrogen or compressed air containing 20% oxygen for 10 min. NiEDDA was synthesized from Nickel (II) hydroxide and ethylenediamine-*N*,*N*′-diacetic acid (*25*) and used at 5 mM. EPR parameters, such as Π accessibilities, were calculated as previously described (*26*, *27*).

Materials. ATP, DTT, and ethylenediamine-*N*,*N*′-diacetic acid were obtained from Sigma Chemical Co. (St. Louis, MO), nickel (II) hydroxide from Aldrich Chemical Co. (Milwaukee, WI), and pyruvate kinase from Roche Molecular Biochemicals (Indianapolis, IN). MTS−SL was obtained from Toronto Research Chemicals (Toronto, Canada). All other reagents were of the highest grade and purity available.

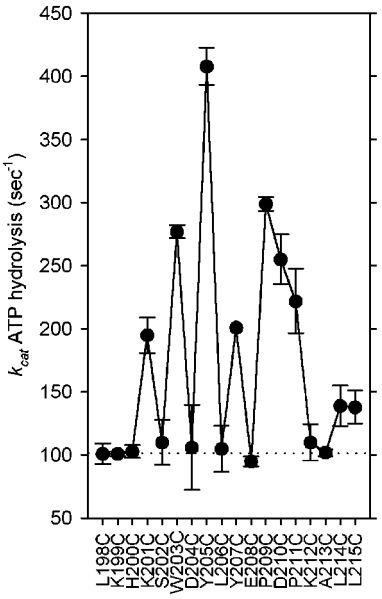

FIGURE 1: k_{cat} of ATP hydrolysis at 30 °C, pH 7.5, for unlabeled F_1 single cysteine mutants from γ198 to γ215. The dotted line indicates the k_{cat} of wild-type F_1, 102 s^{-1}, in this assay. Error bars represent the standard deviation observed over two to six determinations.

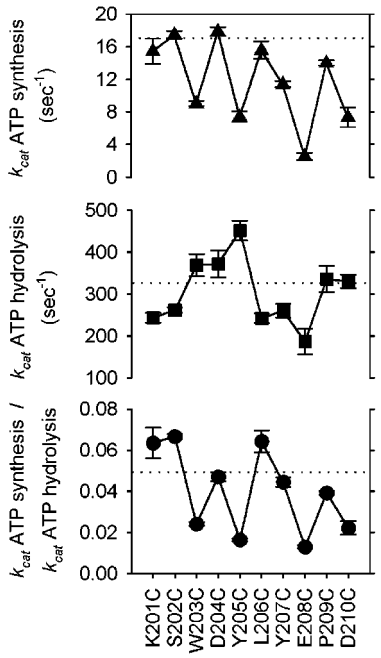

FIGURE 2: Turnovers of ATP synthesis and ATP hydrolysis, and ratio of k_{cat} ATP synthesis to k_{cat} ATP hydrolysis, at 30 °C, pH 7.5, for membranes containing F_OF_1 single cysteine mutants from γ201 to γ210. The dotted lines indicate the values obtained for cysteine-less F_OF_1 in these assays: k_{cat} of ATP synthesis, 17 s^{-1}; k_{cat} of ATP hydrolysis, 324 s^{-1}; and the synthesis:hydrolysis ratio, 0.052, which are comparable to wild-type F_OF_1 (*12*). Error bars represent the standard deviation observed over at least three determinations.

RESULTS

Effect of Cysteine Substitutions on Enzyme Function in F_1 and F_OF_1. The k_{cat} of ATP hydrolysis at 30 °C, pH 7.5 (Figure 1), were determined for purified, unlabeled F_1 enzymes depleted of all 19 native cysteines (*12*) and carrying unique cysteine substitutions at positions γ198 through γ215. Catalytic turnovers of the unlabeled odd-numbered mutants from γ201−208, such as γW203C and γY205C, are 2−4-fold higher, reminiscent of ϵ-depleted F_1, which has high turnover due to the removal of the inhibitory ϵ subunit (*21*, *28*). The pattern disappears towards the amino terminus from position γ200 and toward the carboxyl terminus from position γ210. The γ'/ϵ crystal structure indicates a turn involving γPro209−γAsp210−γPro211 (*10*). The 4-fold increase for γY205C F_1 has been previously reported, in a cysteine replete enzyme (*6*) and in the cysteine depleted F_1 enzyme used herein (*7*). The γY205C−SL F_1, derivatized with MTS−SL as described in Experimental Procedures, has similarly elevated turnover as the underivatized γY205C F_1 mutant enzyme (data not shown).

The ATP synthesis:ATP hydrolysis ratios for F_OF_1 mutants containing cysteines at γ201−210 indicate that cysteine substitution at γ203, γ205, γ208, and γ210 disrupts coupling efficiency in the F_OF_1 complex (Figure 2). In general, the higher catalytic turnovers for ATP hydrolysis observed for many of the soluble mutant F_1 are suppressed in membranous F_OF_1. The k_{cat} for ATP hydrolysis of γY205C F_OF_1 is higher than wild-type as previously reported (*6*, *7*), while that of γE208C is much lower, similar to the γE208K mutant (*8*). Because γE208K and C have similar effects, the results indicate that the glutamate at position γ208 plays a specific role in mediating coupling efficiency.

ATP-driven and NADH-driven ΔpH generated by membranes containing hybrid F_OF_1 reconstituted from spin-labeled γS202C, γD204C, γY205C, or γL206C F_1 are smaller in extent than those for the hybrid F_OF_1 made from the corresponding unlabeled F_1 mutants (compare Figure 3A to C, and 3B to D). The ATP-driven ΔpH for hybrid γS202C and γL206C are comparable to that obtained for hybrid F_OF_1 containing wild-type F_1 (data not shown). In contrast, ATP- and NADH-driven ΔpH for hybrid γD204C indicate that the membranes remain permeable to protons, suggesting that the γ204 cysteine substitution interferes with functional binding of mutant F_1 to F_O, with or without presence of the spin label. The γY205C mutant F_1 binds to F_O because the NADH-driven pumping reconstitutes similar to the γS202C and γL206C mutants, but the spin label appears to interfere with coupling of the ATP-driven proton transport. In all cases, spin-labeled F_1 which has ϵ subunit bound clearly binds to F_O because (i) the spin label that is exclusively on the F_1 associates with the membranes (see below), (ii) binding of F_1 to F_O requires presence of the ϵ subunit (*29*, *30*), and (iii) the labeling efficiency is estimated to be greater than 85%, indicating that the membrane bound activity represents labeled enzyme (see below).

γ198−215 Side Chain Mobility, Accessibility, and Secondary/Tertiary Structure in F_1. To probe the secondary structure of this region of the γ subunit through SDSL analysis of residue side chain mobility and accessibility (*11*), each unique cysteine F_1 mutant was covalently labeled with MTS−SL and analyzed by EPR spectroscopy, including power saturation EPR. The EPR spectra (Figure 4), the ΔH^{-1} reciprocal central line widths (or mobility parameters), and the Π accessibility parameters to the paramagnetic relaxing agents NiEDDA and oxygen (Figure 5) of spin labels attached to cysteines from γ198 to γ215 indicate three different phases of side chain environments.

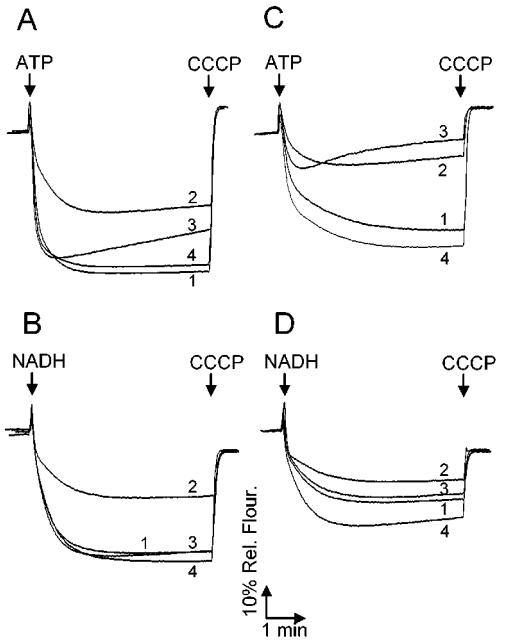

FIGURE 3: Formation of ΔpH, driven by ATP or NADH, in membranes containing hybrid F_OF_1 formed from F_1 single cysteine mutants and wild-type F_O membranes. (A) ATP-driven and (B) NADH-driven ΔpH for membranes containing hybrid F_OF_1 formed from unlabeled F_1 cysteine mutants. Membrane protein was diluted to 0.10 mg/mL in a buffer containing 10 mM HEPES−KOH, 300 mM KCl, 5 mM $MgCl_2$, 1 μM valinomycin, and 1 μM acridine orange, pH 7.5 (*23*). (C) ATP-driven and (D) NADH-driven ΔpH for membranes containing hybrid F_OF_1 formed from spin-labeled F_1 cysteine mutants. 1, γS202C; 2, γD204C; 3, γY205C; 4, γL206C. 1 mM ATP or 2 mM NADH, and 1 μM carbonyl cyanide *m*-chlorophenylhydrazone (final concentrations) were added as indicated by the arrows.

The narrow line shapes and ΔH line widths less than 2.5 G obtained from enzymes with cysteines at positions γLeu198 to γHis200 reflect side chain mobility on the nanosecond time scale (*31*). These nitroxides show high ΔH^{-1} mobilities and high Π NiEDDA and Π oxygen accessibilities, indicating side chain exposure to a polar medium, such as the aqueous bulk solvent. The consistently high mobility and the lack of major variations in these parameters across this short stretch of the γ subunit suggest a mobile, random coil structure.

The spin-labeled cysteines at the even-numbered residue positions from γ201 to γ211 display similarly narrow line shapes (Figure 4), high ΔH^{-1}, high Π NiEDDA and Π oxygen (Figure 5), again signifying side chain exposure to a polar medium. The γE208C mutant was not reactive with MTS−SL (see below). In contrast, the EPR spectra of spin labels attached to cysteines at the odd-numbered positions from γ201 to γ210 show broad line shapes and ΔH line widths of 4.1 to 4.3 G (Figure 4). The low ΔH^{-1}, low Π NiEDDA, and Π oxygen at these positions (Figure 5) indicate that the odd side chains are sterically occluded and restricted by tertiary contact with another protein domain (*32*). The ΔH^{-1} mobilities and Π accessibilities from γ201 to γ209 modulate with a periodicity of two (Figure 5), a pattern previously observed in SDSL of β-sheet proteins (*33*−*36*).

In addition, spectral features in the low field resonances of the even-numbered mutant spectra are similar to low field features of spin-labeled residues on the periphery of β-sheet

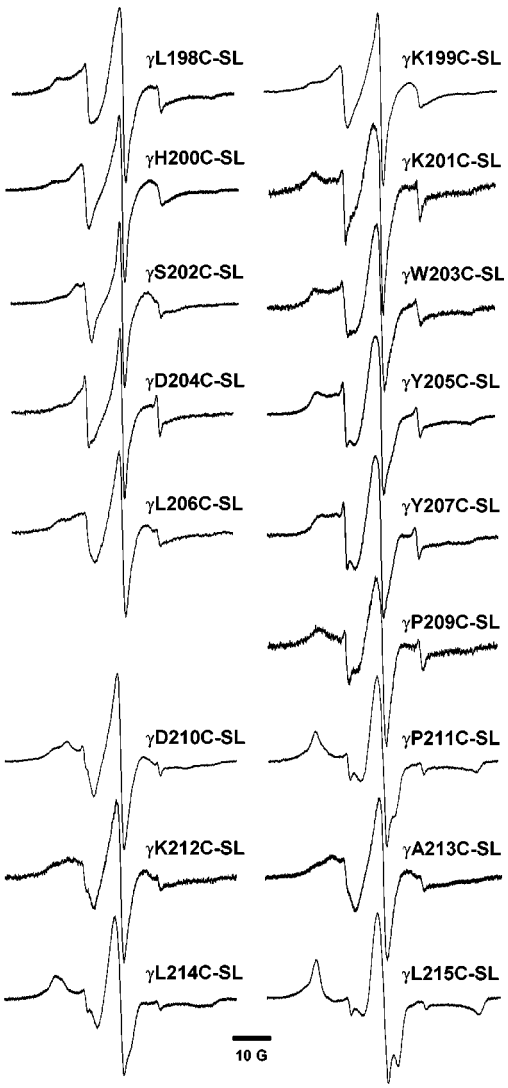

FIGURE 4: EPR spectra of spin-labeled F_1 γ subunit cysteine mutants. The bar represents 10 G.

structures. These features are attributed to motional restriction of the nitroxide by the branching of side chains such as leucine and isoleucine, spatially adjacent on the same face of the β-sheet (*11*). The γ'/ϵ structure places ϵLeu41, ϵLeu42, and ϵThr43 spatially adjacent to γAsp204 and γLeu206 in a similar, although less ordered fashion (*10*).

The EPR spectra and parameters for γK212C−SL and γA213C−SL indicate mobile, solution accessible side chains at these positions. However, the EPR data for γP211C−SL, γL214C−SL, and γL215C−SL indicate steric occlusion, with γP211C−SL and γL215C−SL reporting the lowest ΔH^{-1}, Π NiEDDA, and Π oxygen observed in the entire region. The periodicity in the EPR data from these positions recalls patterns observed in site-directed spin labeling of α-helices (*31*).

The stoichiometry of spin labeling for the 1 h labeling reaction, performed on F_1 used in hybrid F_OF_1 synthesis, was over 85%, and that for the overnight reaction, performed on F_1 samples used in F_1 SDSL studies, was over 95%. Several spectra contain sharp components in the high and low field resonances, indicating the presence of less than 5% unreacted MTS−SL in the samples (Figure 4). Furthermore, a F_1 sample completely lacking cysteines and subjected to the

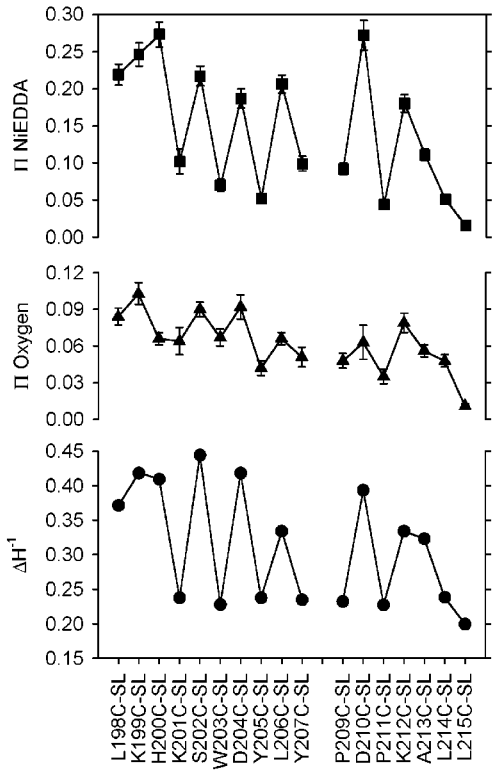

FIGURE 5: ΔH^{-1}, Π oxygen, and Π NiEDDA for F_1 γ subunit cysteine mutants. Values were calculated as previously described (*26*, *27*). Error bars represent the standard error in the power saturation curve fit propagated through the parameter calculations.

MTS−SL labeling procedure showed EPR signal equivalent to 10% or less of the amplitude of the labeled single cysteine mutants (data not shown). This background is comparable to that in other studies (*37*) and is not enough to affect interpretation of the spectra. Control experiments were performed to ensure that labeled cysteine mutant complexes, in particular those with cysteines in the odd-numbered positions, retained bound ϵ subunit. One molar equivalent of recombinant ϵ subunit, with the $(His)_6$ tag removed, added to approximately 40 μM γD204C−SL, γY205C−SL, and γL206C−SL F_1, did not alter the EPR line shapes (data not shown). In a similar manner, we previously reported that the hydrolysis turnover of γY205C F_1 was not significantly inhibited by addition of excess ϵ subunit (*7*).

In contrast to the other mutants, γE208C F_1 was highly resistant to labeling with MTS−SL. Several additional reaction schemes were attempted, including prereduction with 1 mM DTT and labeling in the presence of 1 μM DTT, and prereduction with 2.5 mM tris-(2-carboxyethyl) phosphine (TCEP, Molecular Probes, Eugene, OR) and labeling with 3-maleimido-PROXYL nitroxide (Aldrich Chemical Co., Milwaukee, WI) in the presence of 1 mM TCEP. All of these strategies failed to label γE208C above the EPR signal intensity of the control enzyme containing no cysteines.

γ200−210 Side Chain Mobility and Tertiary Structure in F_OF_1. Spin-labeled F_1 cysteine mutants γH200C−SL, γS202C−SL, γD204C−SL, γY205C−SL, γL206C−SL, and γD210C−SL were bound to F_O-containing membranes at 5:1 molar ratios to create hybrid F_OF_1 complexes, as described in Experimental Procedures. EPR spectroscopy examined the mobility of the nitroxide side chain on the γ subunit during F_1 interactions with F_O (Figure 6). The hybrid

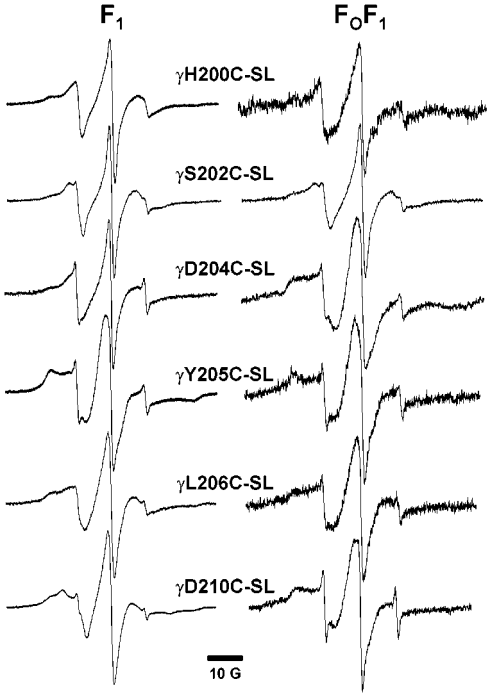

FIGURE 6: EPR spectra of spin-labeled F_1 γ subunit cysteine mutants before and after binding to wild-type F_O membranes to form hybrid F_OF_1 complexes. The bar represents 10 G.

F_OF_1 samples contained low gain EPR signals insufficient for power saturation EPR.

The line widths and line shapes of the EPR spectra of the γH200C−SL, γS202C−SL, γY205C−SL, and γL206C−SL hybrid F_OF_1 constructs did not differ significantly from those of the corresponding spin-labeled F_1 enzymes. The unchanged, high mobilities of the γH200C−SL, γS202C−SL, and γL206C−SL spin-labeled side chains in the hybrid F_OF_1 indicate that these side chains do not contact a protein domain in F_O or F_1. The γY205C−SL spin-labeled side chain fully contacts domains in F_1, and the low mobility does not change upon binding to F_O. The other odd-numbered mutants were not tested. In contrast, the ΔH line widths of γD204C−SL and γD210C−SL increased 1.8 and 1.3 G, respectively, upon binding to F_O, with an amplitude increase in the low field resonance indicative of motion restriction (*31*). The reduced mobilities of the γD204C−SL and γD210C−SL side chains indicate a specific tertiary contact, probably with the *c* subunits, upon association with F_O.

DISCUSSION

Structural Assignments of the γ Subunit in the $\gamma-\epsilon-$c Interface. The periodicity of two in the EPR data and the alternating polarity in the accessibilities from γLys201 to γTyr207 demonstrates a biphasically ordered strand, with the even side chains on the periphery of the F_1 complex projecting into solution, and the odd side chains contacting an F_1 domain involved in ϵ inhibition. Several of the EPR spectra contain line shape features characteristic of the EPR line shapes from test-case SDSL of β-sheet proteins (*11*). The γ'/ϵ structure *(10)* indicates two parallel β sheet-type hydrogen bonds, γLeu206−ϵLeu42 and γGlu208−ϵLeu42. The periodicity in the SDSL data, the EPR line shapes, and the β-sheet hydrogen bonds support our proposal that γ201−208 is a β-strand.

The high mobility and solution accessibility of γLeu198 to γHis200 indicate that this region is a random coil on the periphery of the γ subunit. The failure of the γ′/ϵ structure (*10*) to resolve γ191−198 also suggests a dynamic conformation in this region, under the crystallization conditions. The EPR data for γP211C−SL to γL215C−SL show the start of an α-helical periodicity in these side chain environments. The resolution of helical electron density for this region in the γ′/ϵ structure (*10*) and in a structure of the full *E. coli* F_1 complex (*38*) show that the EPR data represent the beginning of the carboxyl-terminal α-helix of the γ subunit catalytic rotor after the turn formed by γPro209−γAsp210−γPro211 (see below).

Roles of γ201−211 Side Chains in Mediating ϵ Subunit Inhibition and Modulation of Catalysis. The increased ATP hydrolytic rates of the cysteine mutants of the odd-numbered positions from γ201−211 indicate that these side chains affect the interactions that mediate ϵ subunit inhibition, and the EPR data at these positions show tertiary contact with an adjacent domain in F_1. The proximity of the odd residue side chains and the ϵ subunit, previously indicated by high yield cross-linking of γY205C and γY207C to ϵH38C and ϵT43C (*6*, *39*) and the γ′/ϵ structure (*10*), identifies this adjacent domain as the ϵ subunit. The γ subunit cysteine substitutions disrupt the functional interactions at these positions to varying degrees, perhaps through gross structural perturbations, or through disruption of specific side chain interactions with the adjacent domain. The former possibility is not likely because all 18 cysteine mutants were assembled in the membrane, and purification yields were similar to wild type. These results suggest that F_1 affinity for F_O was not significantly altered by cysteine substitution at any of these positions, as the F_1 purification depends on a stable F_OF_1 complex. More likely, the cysteine substitution disrupts specific interactions between the two subunits.

The two largest reductions in ϵ inhibition are observed for γW203C and γY205C in F_1. The same two substitutions also significantly reduce coupling efficiency between transport and catalysis in F_OF_1. While γK201C and γY207C also have increased ATP hydrolysis rates in F_1, association with F_O suppresses their effects and γK201C and γY207C F_OF_1 have normal coupling efficiency. The effects of the cysteine substitution at these position were not as severe as at γ203 and γ205.

Previously, we have implicated the ϵ inhibition in modulating the rotational catalytic mechanism in a manner that is critical for achieving maximum coupling efficiency (*7*). Linear free energy analysis of the temperature dependence of the k_{cat} for ATP hydrolysis of the γY205C mutant enzyme as well as other complexes abrogated of ϵ inhibition indicates that these enzymes have a different transition state structure for steady-state catalysis (*7*). Importantly, the loss of ϵ inhibition correlates with decreased coupling efficiency. In fact, the γW203C enzyme, which has low coupling efficiency, has the same transition state structure as γY205C, while γY207C, which has wild-type coupling, does not (data not shown). These results reinforce our hypothesis that the ϵ inhibition is a modulatory activity that coordinates the catalytic transition state to that of transport and is critical for high efficiency coupling.

The odd-numbered side chains γLys201, γTrp203, γTyr205, and γTyr207 are bulky and mostly hydrophobic functional groups. The effects of the cysteine substitutions suggest that ϵ inhibition is mediated through this region by a combination of hydrophobic and steric interactions. The wild-type levels of ATP hydrolysis rates of γ198−200, the even-numbered γ201−208 substitutions, and γ212−215 indicate that these residues are not involved in ϵ inhibition.

According to the γ′/ϵ structure (*10*), γPro209−Asp210−Pro211 forms a turn between the γ−ϵ interface and the beginning of the long carboxyl terminal α-helix that forms the rotor of the catalytic mechanism. Even though the Pro−X−Pro motif is common in turns (*40*) and a similar motif is found in many γ subunit sequences, it is not conserved. The sequence variability probably reflects conformational differences in this region which must match the interacting structure and dynamics of the ϵ and *c* subunits. The high ATP hydrolysis rates of the cysteine mutants in all three positions of the turn may signify perturbation of the backbone; however, the γP209C F_OF_1 has normal coupling function (Figure 2). Interestingly, the effects of replacing this proline are suppressed upon association with F_O. Only the cysteine in place of γAsp210 disrupts coupling efficiency. Significantly, the γ′/ϵ structure and the EPR data indicate that the side chain of γAsp210 projects into aqueous solution with no protein contacts; however, upon binding to F_O, its mobility and tertiary contact change significantly indicating an interaction with an F_O subunit, probably subunit *c*. We note that two acidic residues in this region, γAsp204 and γAsp210, have been found to contact F_O or have been implicated in communication of coupling information with the F_O. While the third acidic residue, γE208C, was not available to the spin label, second site mutations in the polar loop of the *c* subunit suppress the deleterious effects of γE208K indicating its functional interaction with the transport domain (*8*). The distance between these residues and the opposing projections of their side chains in the γ′/ϵ structure (*10*) suggest that the three residues interact with polar loops from different *c* subunits.

ACKNOWLEDGMENT

We thank Drs. David Cafiso and Eduardo Perozo for spectrometer time and many helpful discussions.

REFERENCES

1. Noji, H., Yasuda, R., Yoshida, M., and Kinosita, K. (1997) *Nature 386*, 299−302.
2. Kato-Yamada, Y., Noji, H., Yasuda, R., Kinosita, K., and Yoshida, M. (1998) *J. Biol. Chem. 273*, 19375−19377.
3. Sambongi, Y., Iko, Y., Tanabe, M., Omote, H., Iwamoto-Kihara, A., Ueda, I., Yanagida, T., Wada, Y., and Futai, M. (1999) *Science 286*, 1722−1724.
4. Nakamoto, R. K., Ketchum, C. K., and Al-Shawi, M. K. (1999) *Annu. Rev. Biophys. Biomol. Struct. 28*, 205−234.
5. Nakamoto, R. K., Ketchum, C. J., Kuo, P. H., Peskova, Y. B., and Al-Shawi, M. K. (2000) *Biochim. Biophys. Acta 1458*, 289−299.
6. Watts, S. D., Tang, C., and Capaldi, R. A. (1996) *J. Biol. Chem. 271*, 28341−28347.
7. Peskova, Y. B., and Nakamoto, R. K. (2000) *Biochemistry 39*, 11830−11836.
8. Ketchum, C. J., and Nakamoto, R. K. (1998) *J. Biol. Chem. 273*, 22292−22297.
9. Gibbons, C., Montgomery, M. G., Leslie, A. G. W., and Walker, J. E. (2000) *Nat. Struct. Biol. 7*, 1055−1061.
10. Rodgers, A. J. W., and Wilce, M. C. J. (2000) *Nat. Struct. Biol. 7*, 1051−1054.

11. Hubbell, W. L., Gross, A., Langen, R., and Lietzow, M. A. (1998) *Curr. Opin. Struct. Biol. 8*, 649−656.
12. Kuo, P. H., Ketchum, C. J., and Nakamoto, R. K. (1998) *FEBS Lett. 426*, 217−220.
13. Klionsky, D. J., Brusilow, W. S. A., and Simoni, R. D. (1984) *J. Bacteriol. 160*, 1055−1060.
14. Mullis, K. B., Ferre, F., and Gibbs, R. A. (1994) *The Polymerase Chain Reaction*, Birkhauser, Boston.
15. Sheffield, P. J., Derewenda, U., Taylor, J., Parsons, T. J., and Derewenda, Z. S. (1999) *Acta Crystallogr. Sect. D-Biol. Cryst. 55*, 356−359.
16. Sambrook, J., Fritsch, E. F., and Maniatis, T. (1989) *Molecular Cloning: A Laboratory Manual*, 2nd ed., Cold Spring Harbor Laboratory Press, Cold Spring Harbor.
17. Tanaka, S., Lerner, S. A., and Lin, E. C. C. (1967) *J. Bacteriol. 93*, 642−648.
18. Futai, M., Sternweis, P. C., and Heppel, L. A. (1974) *Proc. Natl. Acad. Sci. U.S.A. 71*, 2725−2729.
19. Laemmli, U. K. (1970) *Nature 227*, 680−685.
20. Lowry, O. H., Rosebrough, N. J., Farr, A. C., and Randall, R. J. (1951) *J. Biol. Chem. 193*, 265−275.
21. Al-Shawi, M. K., Ketchum, C. J., and Nakamoto, R. K. (1997) *J. Biol. Chem. 272*, 2300−2306.
22. Al-Shawi, M. K., Ketchum, C. J., and Nakamoto, R. K. (1997) *Biochemistry 36*, 12961−12969.
23. Nakamoto, R. K., Al-Shawi, M. K., and Futai, M. (1995) *J. Biol. Chem. 270*, 14042−14046.
24. Penefsky, H. S. (1979) *Methods Enzymol. 56*, 527−530.
25. Altenbach, C., Greenhalgh, D. A., Khorana, H. G., and Hubbell, W. L. (1994) *Proc. Natl. Acad. Sci. U.S.A. 91*, 1667−1671.
26. Farahbakhsh, Z. T., Hideg, K., and Hubbell, W. L. (1992) *Photochem. Photobiol. 56*, 1019−1033.
27. Altenbach, C., Yang, K., Farrens, D. L., Farahbakhsh, Z. T., Khorana, H. G., and Hubbell, W. L. (1996) *Biochemistry 35*, 12470−12478.
28. Sternweis, P. C., and Smith, J. B. (1980) *Biochemistry 19*, 526−531.
29. Futai, M. (1977) *Biochem. Biophys. Res. Commun. 79*, 1231−1237.
30. Dunn, S. D., and Futai, M. (1980) *J. Biol. Chem. 255*, 113−118.
31. Mchaourab, H. S., Lietzow, M. A., Hideg, K., and Hubbell, W. L. (1996) *Biochemistry 35*, 7692−7704.
32. Perozo, E., Cortes, D. M., and Cuello, L. G. (1998) *Nat. Struct. Biol. 5*, 459−469.
33. Koteiche, H. A., Berengian, A. R., and Mchaourab, H. S. (1998) *Biochemistry 37*, 12681−12688.
34. Berengian, A. R., Bova, M. P., and Mchaourab, H. S. (1997) *Biochemistry 36*, 9951−9957.
35. Mchaourab, H. S., Berengian, A. R., and Koteiche, H. A. (1997) *Biochemistry 36*, 14627−14634.
36. Glasgow, B. J., Gasymov, O. K., Abduragimov, A. R., Yusifov, T. N., Altenbach, C., and Hubbell, W. L. (1999) *Biochemistry 38*, 13707−13716.
37. Gross, A., Columbus, L., Hideg, K., Altenbach, C., and Hubbell, W. L. (1999) *Biochemistry 38*, 10324−10335.
38. Hausrath, A. C., Gruber, G., Matthews, B. W., and Capaldi, R. A. (1999) *Proc. Natl. Acad. Sci. U.S.A. 96*, 13697−13702.
39. Watts, S. D., and Capaldi, R. A. (1997) *J. Biol. Chem. 272*, 15065−15068.
40. MacArthur, M. W., and Thornton, J. M. (1991) *J. Mol. Biol. 218*, 397−412.

BI0155697